

## Probing the Geometry and Interconnectivity of Pores in Organic Aerogels Using Hyperpolarized $^{129}\text{Xe}$ NMR Spectroscopy

I. L. Moudrakovski, L.-Q. Wang,<sup>\*,†</sup> T. Baumann,<sup>‡</sup> J. H. Satcher, Jr.,<sup>‡</sup> G. J. Exarhos,<sup>†</sup>  
C. I. Ratcliffe, and J. A. Ripmeester

*Steele Institute for Molecular Sciences, National Research Council, Ottawa, Ontario, Canada K1A 0R6,  
Material Science Department, Pacific Northwest National Laboratory, Richland, Washington 99352,  
Chemistry and Material Science Directorate, Lawrence Livermore National Laboratory, Livermore, California 94550*

Received January 23, 2004; E-mail: lq.wang@pnl.gov

Aerogels represent a class of novel open-pore materials with high surface area and nanometer pore sizes. They exhibit very low mass densities, low thermal conductivity, good acoustic insulation, and low dielectric constants. The materials have potential applications in catalysis, advanced separation techniques, energy storage, environmental remediation, and as thermal insulators. Organic aerogels are stiffer and stronger than silica aerogels and are better insulators with higher thermal resistance. Resorcinol–formaldehyde (RF) aerogels are typically prepared through the base-catalyzed sol–gel polymerization followed by drying in supercritical  $\text{CO}_2$ .<sup>1,2</sup> The [resorcinol]/[catalyst] ( $R/C$ ) ratio of the starting sol–gel solution has been determined to be the dominant factor that affects the properties of RF aerogels. Since the unique microstructures of aerogels are responsible for their unusual properties, characterizing the detailed porous structures and correlating them with the processing parameters are vital to establish rational design principles for novel organic aerogels with tailored properties. In this communication we report the first use of hyperpolarized (HP)  $^{129}\text{Xe}$  NMR to probe the geometry and interconnectivity of pores in RF aerogels and to correlate these with synthetic conditions. Our work demonstrates that HP  $^{129}\text{Xe}$  NMR is thus far the only method for accurately measuring the free volume-to-surface-area ( $V_g/S$ ) ratios for soft mesoporous materials without using geometric models.

RF aerogels with  $R/C$  ratios of 50, 100, 200, 300, and 500 were prepared following procedures described previously.<sup>1</sup>  $^{129}\text{Xe}$  continuous flow (CF) HP NMR spectra taken at room temperature for all samples show two signals in addition to the gas line near 0 ppm. Figure 1a displays a representative spectrum for RF with  $R/C = 300$ . On the basis of the magnitude of the chemical shifts (CS) and variation of the shifts with the temperature, we attribute the broad signal at 140 ppm to the micropores formed by agglomerated polymer particles and a narrow signal at 90 ppm to the mesopores.  $^{129}\text{Xe}$  2D EXSY spectra (Figure 1b–d) reveal the interconnectivity between different adsorption regions. In  $^{129}\text{Xe}$  2D EXSY experiments,<sup>3–6</sup> the exchange between regions with different CSs manifests itself in the appearance of cross-peaks between the signals from the sites in exchange. The intensities of the cross-peaks are proportional to the exchange time ( $\tau$ ) set in the experimental pulse sequence. For the sites without exchange, or when the exchange time  $\tau$  is set to zero, only intensity on the main diagonal will appear in the spectrum. As expected, with  $\tau = 0$  the signals appear only on the main diagonal. Off-diagonal intensities, however, appear even at  $\tau = 0.5$  ms and become quite pronounced with  $\tau > 1$  ms. The 2D EXSY spectra show that on a time scale of a few milliseconds there is exchange between all the adsorption regions and xenon in the gas phase. However, there is a striking difference between the

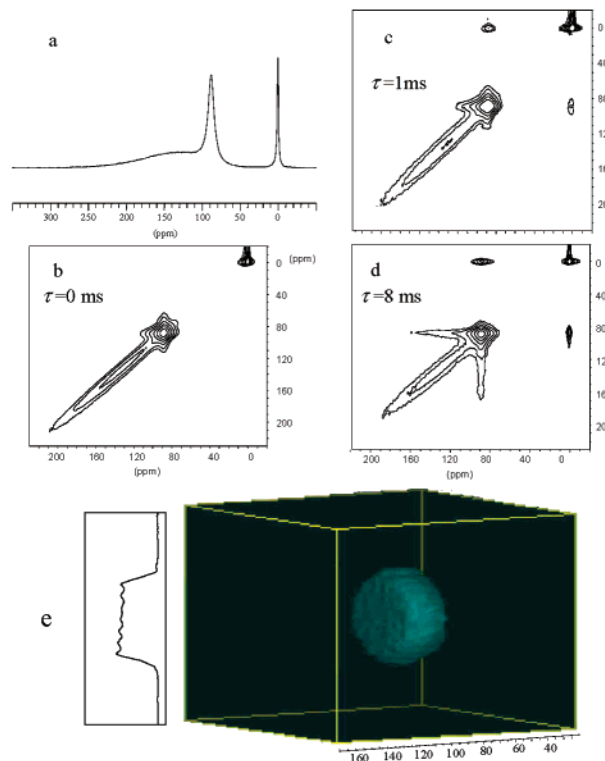


**Figure 1.** (a) CF HP  $^{129}\text{Xe}$  NMR spectra for RF aerogels prepared with an  $R/C$  ratio of 300. (b–d) CF HP 2D EXSY  $^{129}\text{Xe}$  NMR spectra for RF aerogels ( $R/C = 300$ ) recorded with  $\tau$  as indicated. All spectra were obtained at 293 K with a HP Xe flow rate of 45 sccm. (e) CF  $^{129}\text{Xe}$  Chemical Shift image of Xe in cylindrical block of RF aerogel ( $R/C = 300$ ). Intensity profile shown on the left is taken through the center of the image.

shapes of the signals. The diagonal signals from the gas phase and from adsorbed xenon ( $\sim 90$  ppm) each have 2D line shapes with cylindrical symmetry. This, however, is not the case for the broader component which appears as a long and narrow ridge. This feature indicates a broad distribution of adsorption sites with very slow exchange between different parts of this subset. Overall, the observed evolution with  $\tau$  clearly indicates a hierarchical set of exchange processes. The exchange of Xe gas follows the sequence (from fastest to slowest): mesopores with free gas, gas in meso- and micropores, free gas with micropores, and finally, among micropore sites. This order is a good indication of a rather homogeneous distribution of micropores throughout the material where large micropore domains do not exist as isolated entities. In such cases the accessible micropores are always open either to mesopores or to free xenon, and obviously it takes longer for a xenon atom to exchange between two different micropores than between micropores and mesopores or free gas.

<sup>†</sup> Pacific Northwest National Laboratory.

<sup>‡</sup> Lawrence Livermore National Laboratory.

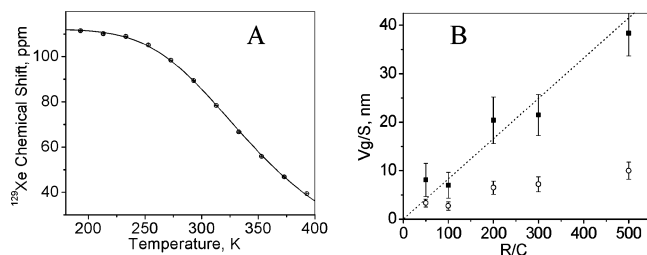


**Figure 2.** (A) The  $^{129}\text{Xe}$  chemical shift plotted as a function of temperature for the narrow signal arising from the mesopores in RF aerogels ( $R/C = 300$ ). The solid dots are experimental data obtained from CF HP  $^{129}\text{Xe}$  NMR spectra recorded at 20 K intervals, and the solid line is the fit using eq 1. (B) The volume to surface-area ratio  $V_g/S$  as a function of  $R/C$  ratios from Xe NMR (■) and  $\text{N}_2$  adsorption data (○).

The homogeneity of distribution of the mesopores in the aerogels can be tested directly using CF  $^{129}\text{Xe}$  chemical shift imaging,<sup>7</sup> as shown in Figure 1e. The evenness of the profile clearly indicates uniformity of distribution of the mesoporous spaces throughout the bulk of aerogel.

Temperature-dependent CS data can be used to extract the physical parameters related to the adsorption properties of materials. Variations in the  $^{129}\text{Xe}$  CS's with temperature for the mesopore component in the spectra are summarized in Figure 2A. The observed changes are characteristic of the physical adsorption of xenon on solid surfaces, as observed before in numerous micro- and mesoporous materials.<sup>8,9</sup> One can fit the temperature-dependent CS data to extract the parameters related to the adsorption properties of the materials.<sup>8</sup> In the fast exchange approximation with weak adsorption the temperature dependence of the observed CS  $\delta$  for arbitrary pores can be expressed as:<sup>8</sup>

$$\delta = \delta_s \left( 1 + \frac{V_g}{SK_0RT} e^{-\Delta H_{\text{ads}}/RT} \right)^{-1} \quad (1)$$

where  $V_g$  is the free volume inside the aerogel,  $S$  is a specific surface area,  $K_0$  is the pre-exponent of Henry's constant,  $R$  is the universal gas constant,  $\Delta H_{\text{ads}}$  is the heat of adsorption and  $\delta_s$  is the  $^{129}\text{Xe}$  CS characteristic of the surface.  $K_0$  was found from Xe adsorption data (Supporting Information), and  $\delta_s$ ,  $\Delta H_{\text{ads}}$ , and  $V_g/S$  were then determined from fits of the variable temperature mesopore CS measurements to eq 1, as shown in Figure 2A. All observed  $\Delta H_{\text{ads}}$ 's are close to 20 kJ/mol, consistent with physical adsorption of Xe.  $\delta_s$ 's are similar for all the samples and comparable to those normally observed on uncharged surfaces of silica- or silica-organic-based materials.<sup>9</sup> A similar analysis for the broad signal from the micropores was not carried out, since this would be somewhat ambiguous due to the fact that the signal represents a distribution of micropores.

The experimentally determined volume-to-surface-area ratios ( $V_g/S$ ) were found to show a very strong correlation with the  $R/C$  ratios (Figure 2B), with an unusually large span in the observed values; an increase in  $R/C$  ratio from 50 to 500 inducing about 5-fold rise in the  $V_g/S$ 's. Since the chemical composition of the surface is practically identical for all the samples, chemical effects can be ruled out, consistent with the absence of variation in  $\delta_s$ . It is only the change in the geometry, size, and interconnectivity of the voids that should be responsible for the observed changes in  $V_g/S$ . What makes the situation particularly interesting is the magnitude of the  $V_g/S$  change. From simple geometrical considerations one can easily show that the observed changes in  $V_g/S$  cannot be reproduced from a single model, and will necessarily require some significant rearrangements of the void spaces, whether by some additional connectivity between the pores, changing the shape of the pores, or drastic repacking of the materials framework. As an illustration, in a simple case of cylindrical or slit pores the interconnection of

the pores can increase  $V_g/S$  by no more than a factor of 2.<sup>8</sup> Even more advanced models, i.e., a globular model with quite open void space,<sup>10</sup> is unlikely to account for such a large span of  $V_g/S$  as observed in the present study. The ratio of total free volume to total surface area obtained from  $\text{N}_2$  adsorption data (Figure 2B and Supporting Information) displays a weaker correlation with the  $R/C$  ratio than the  $V_g/S$  of the mesoporous space sampled by Xe atoms, indicating that the  $R/C$  ratio has a large effect on the mesoporous region.

The increase in  $V_g/S$  with  $R/C$  in the current system is mainly due to a decrease in the surface of the accessible void space and not due to a decrease in the density of the material. Although the catalyst concentration does have some effect on the density, the latter parameter does not correlate with  $R/C$  the same way as  $V_g/S$  and, in fact, is practically constant for an  $R/C$  ratio above 100.<sup>11</sup> This implies that for materials prepared with smaller  $R/C$  ratios the framework will be composed of smaller particles and the accessible voids on the average will be smaller, providing a higher surface area. If the average density remains nearly the same, then an increase in  $V_g/S$  with  $R/C$  indicates large average particle sizes (and smaller surface area), and on average larger voids as well. These conclusions agree well with TEM data for RF aerogels prepared with different  $R/C$  ratios.<sup>11</sup>

In conclusion, we have demonstrated that HP  $^{129}\text{Xe}$  NMR is an ideal means for assessing the volume-to-surface-area ( $V_g/S$ ) ratios of mesopores in organic aerogels without using any geometric models. Both this ratio and the Xe exchange data provide important insights into the geometry and the interconnectivity of the nano- and mesoporous spaces in these soft materials. Once again this demonstrates the power and complementarity of HP  $^{129}\text{Xe}$  NMR spectroscopy versus conventional techniques in providing new insights into pore structure.

**Acknowledgment.** This work was partly supported by the Division of Materials Sciences, Office of Basic Energy Sciences and Engineering, U.S. Department of Energy (USDOE). Pacific Northwest National Laboratory is a multiprogram national laboratory operated for the USDOE by Battelle Memorial Institute under Contract DE-AC06-76RL0 1830.

**Supporting Information Available:** Physical properties of RF aerogels. This material is available free of charge via the Internet at <http://pubs.acs.org>.

## References

- (1) Pekala, R. W. *J. Mater. Sci.* **1989**, *24*, 3221.
- (2) (a) Pekala, R. W.; Alviso, C. T.; Kong, F. M.; Hulsey, S. S. *J. Non-Cryst. Solids* **1992**, *145*, 90. (b) Pekala, R. W.; Alviso, C. T.; LeMay, J. D. In *Chemical Processing of Advanced Materials*; Hensch, L. L., West, J. K., Eds.; J. Wiley & Sons: New York, 1992; p 671. (c) Kong, F. M.; LeMay, J. D.; Hulsey, S. S.; Alviso, C. T.; Pekala, R. W. *J. Mater. Sci.* **1993**, *8*, 3100.
- (3) Larsen, R. G.; Shore, J. S.; Schmidt-Rohr, K.; Emsley, L.; Long, H.; Janicke, M.; Chmelka, B. F.; Pines, A. *Chem. Phys. Lett.* **1993**, *214*, 220.
- (4) Kritzenberger, J.; Gaede, H. C.; Shore, J.; Pines, A. *J. Phys. Chem.* **1994**, *98*, 10173.
- (5) (a) Moudrakovski, I. L.; Ratcliffe, C. I.; Ripmeester, J. A. *J. Am. Chem. Soc.* **1998**, *120*, 3123. (b) Moudrakovski, I. L.; Ratcliffe, C. I.; Ripmeester, J. A. *Appl. Magn. Res.* **1995**, *8*, 385. (c) Zhu, X.; Moudrakovski, I. L.; Ripmeester, J. A. *Energy Fuels* **1997**, *11*, 245.
- (6) Kentgens A. P. M.; van Boxtel, H. A.; Verweel, R. J. *Macromolecules* **1991**, *24*, 3712.
- (7) (a) Gregory, D. M.; Gerald, R. E., II; Botto, R. E. *J. Magn. Reson.* **1998**, *131*, 327. (b) Moudrakovski, I.; Lang, S.; Ratcliffe, C. I.; Santyr, G.; Ripmeester, J. A. *J. Magn. Res.* **2000**, *144*, 372.
- (8) Terskikh, V.; Moudrakovski, I.; Mastikhin, V. *J. Chem. Soc., Faraday Trans.* **1993**, *89*, 4239.
- (9) Terskikh, V. V.; Moudrakovski, I. L.; Breeze, S. R.; Lang, S.; Ratcliffe, C. I.; Ripmeester, J. A.; Sayari, A. *Langmuir* **2002**, *18*, 5653.
- (10) Karnaukhov, A. P. *Kinet. Katal.* **1971**, *12*, 1025.
- (11) LeMay, J. D.; Hopper, R. W.; Hrubesh, L. W.; Pekala, R. W. *MRS Bull.* **1990**, *15*, 30.

JA049577X